ESRF	**Experiment title: Dynamics of self-assembled organic nanotubes**	**Experiment number**: SC-2559
Beamline: ID10C	**Date of experiment**: from: 22/10/2008 to: 28/10/2008	**Date of report**: 24/02/2009
Shifts: 18	**Local contact**: Lutz Wiegart	*Received at ESRF:*

Names and affiliations of applicants (* indicates experimentalists):

Pierre TERECH* (CEA/CNRS Grenoble)

Chiara CARONNA* (ESRF)

Shreedhar Bhat*

Agnès Duri (INRA, Montpellier)

Report:

Introduction. We report a X-ray Photon Correlation Spectroscopy (XPCS) and Small Angle X-ray Scattering (SAXS) experiment on gels of self-assembled organic nanotubes.

Dispersing lithocholic bile acid (LCA) in aqueous solutions of sodium hydroxide or ammonia leads to the formation of organic nanotubes with well-defined diameters on the nanometer scale, exhibiting a remarkable cross-sectional monodispersity. The suspensions appear to be tuneable from liquid- to solid-like via the LCA concentration. In solution, the tubes show a remarkable ease for a parallel orientation with respect to each. The length of the tubes can be varied via the temperature: upon increasing the temperature the statistical length decreases and favours in return, the formation of highly hexagonally ordered bundles up to a certain temperature threshold above which decomposition occurs.

The main experimental challenges in this study are related to (i) the relatively fast dynamics with decay times of the orders of one second in combination with (ii) a rather weak scattering signal originating solely from the organic entities, and (iii) the control and *in-situ* monitoring of the geometrical parameters of the nanotubes.

Materials and Methods. Samples of LCA in aqueous dispersions of ammonia and sodium hydroxide were studied in the concentration range from 3.7 %w/w to 5% w/w LCA content. Such samples were found to be adapted to the XPCS measurements due to their scattering power and the timescales of their dynamics. Experiments were carried out at 20°C and at 45°C were the formation of hexagonally ordered bundles is expected. The samples were filled in quartz capillaries of 1.5 mm diameter which were hosted in a copper holder. The whole assembly was surrounded by an insulation vacuum to increase the temperature stability and minimize parasitic air scattering. Heating and cooling of the sample was achieved via peltier elements controlled by a Lakeshore PID controller. The such obtained temperature stability was ±0.005°C. The X-ray radiation of two U27 undulators was focused by Be compound refractive lenses and monochromatized to an energy of 8.03 keV (λ=0.154 nm) by means of a Si(111) pseudo-channel cut monochromator. A partially coherent beam was defined by a 20 x 20µm² aperture and the resulting Frauenhofer fringes were cut by a

subsequent guard slit. The achieved flux was of the order of 10^{10} photons/second. The XPCS setup used either a CCD detector (Princeton, 22.5 x 22.5 µm² pixel size, minimum lag time ~1 second) or a pixel detector (Medipix, 55 x 55 µm² pixel size, 1 kHz full frame rate). Both detectors were mounted in parallel on a linear translation at a sample detector distance of ~2400 mm, to be easily exchangeable according to the sample dynamics. This setup provided a q-range for the dynamics measurements from 0.017 to 0.22 nm^{-1} (CCD) and from 0.017 to 0.12 nm^{-1} (Medipix), respectively. A tungsten rod of 2 mm diameter glued to a 13 µm thick Kapton foil was used as a central beam stop allowing to record the full scattering pattern over an angular range of 2π. The second setup for the SAXS measurements up to larger q vectors employed a Frelon camera (46 x 46 µm² pixel size) with a proxytronic image amplifier, placed on the theta arm of the ID10C diffractometer at a sample distance of 950 mm (q-range: 0.09 to 2.01 nm^{-1}) and a 3 x 3 mm central beamstop. Changing between the two setups was possible within a couple of minutes without need for realignments.

Results. The dynamics was measured for various samples in the concentration range between 3.75 and 5 %w/w. The two times correlation functions were calculated from the time-resolved series of speckle pattern according to the formula $g_2(q,t,\tau) = \langle I(q,t)I(q,t+\tau)\rangle / \langle I(q,t)\rangle\langle I(q,t+\tau)\rangle$, where the average is performed over pixels with the same wavevector transfer q. In the phase at 20°C this two-times correlation function of e.g. a sample with 3.75 %w/w of LCA in aqueous ammonia solution didn't show time dependent dynamics such as for instance aging or heterogeneities. Therefore the ergodic time average of the correlation functions were calculated as $g_2(q,\tau) = \langle I(q,t)I(q,t+\tau)\rangle_t / \langle I(q,t)\rangle_t^2$. Typical correlation functions are shown in figure 1 a).

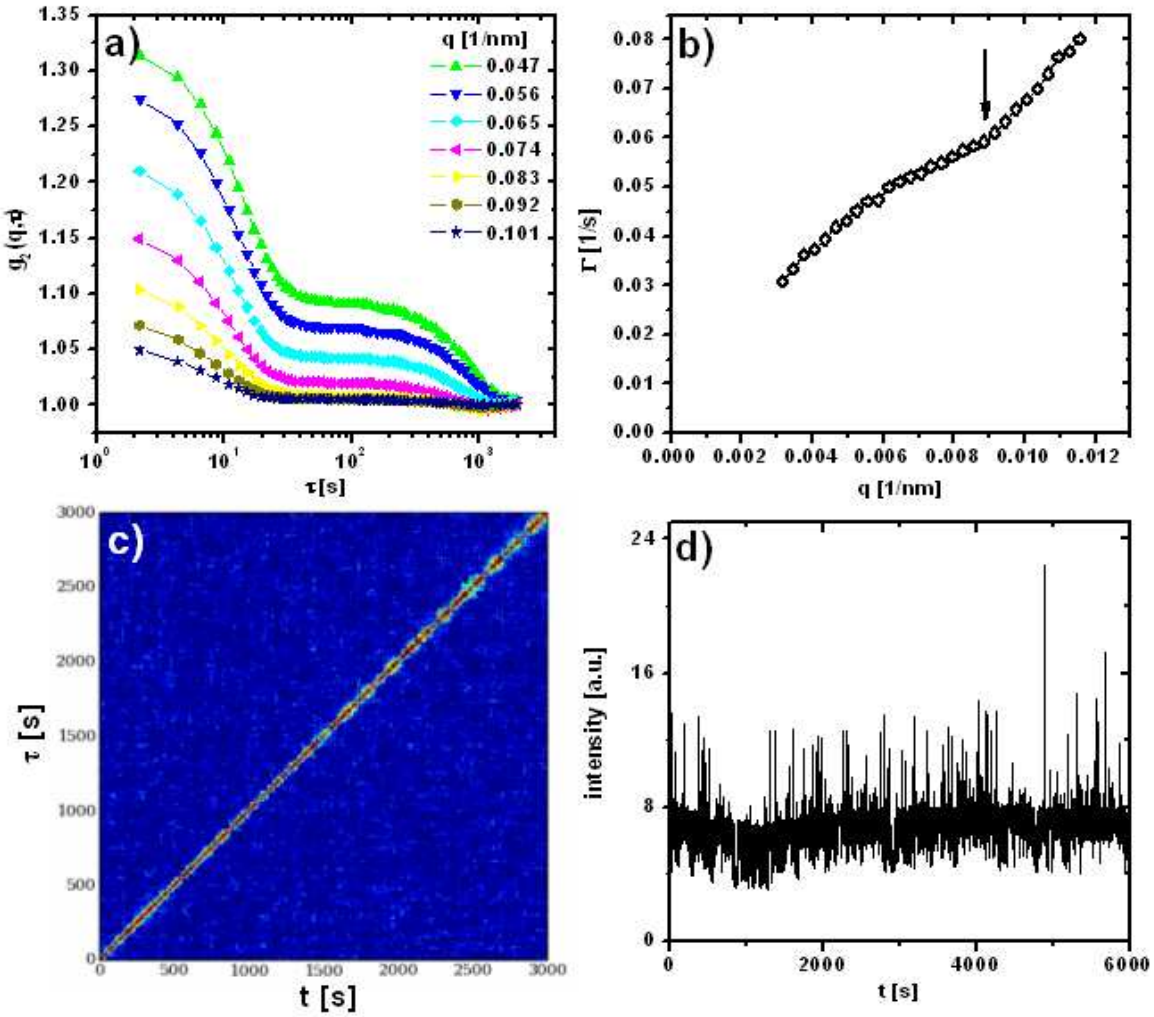

Figure 1. a) time averaged correlation functions for 3.74% w/w nanotube suspensions at T=20°C. b) relaxation rate obtained by fitting the fast decay of the correlation functions shown in a), the arrow indicated the slowing down of the dynamics around q=0.09 nm^{-1}. c) two times correlation function showing dynamics heterogeneities for a 5% w/w nanotube suspensions at T=45°C. d) jitter in the q-averaged intensity due to faulty shutter triggering.

The dynamics is characterized by a fast decay in the order of seconds and a second decay in the order of hundreds of seconds. We tentatively assign the first decay to the translational diffusion of the cylinders within the network while the second one might be associated with the rotational, end-over-end motion of the cylinders. Fitting the first decay with a compressed exponential decay of the form $g_2(\tau) = a\exp(-\Gamma\tau)^{\gamma} + b$ leads to the relaxation rates presented in figure 1 b). The compression exponent γ was thereby found to take values between 1.2 and 1.6. The slope of $\Gamma(q)$ shows a distinct deviation from a q^2 behaviour, indicating that the underlying dynamics is more complicated than simple Brownian diffusion of rod-like particles in a surrounding liquid. A slowing down in the dynamics is observed around a wavevector transfer of ~0.09 nm-1 (indicated by an arrow in figure 1 b)). The corresponding length scale in real space is about 70 nm and thus of the same order as the outer diameter of the cylindrical tubes. The observed change in the dynamics might be therefore related to the effect of DeGennes-narrowing. Contrary, the dynamics of a sample made of 5 %w/w LCA in aqueous NaOH at a temperature of 45°C was found to be governed by heterogeneities. The corresponding two-times correlation function is shown in figure 1 c).

In conclusion, the rather complicated dynamics of the system requires a systematic study as a function of the counter ion (NH_4^+/Na^+), concentration of LCA (in the range 3.7 to ~7 %w/w) and temperature, in order to enable more elaborate analysis of the different features. Unfortunately, many data sets taken during the experimental run reported here cannot be used for a reliable data analysis, because they are polluted by jitter arising from (i) faulty triggering of the fast shutter located before the sample, resulting in a bad synchronization with the CCD detector, (ii) a network overload resulting in CCD images being saved with variable and unknown lag times, (iii) a bug in the firmware update of the Medipix detector. Typical jitter is reported in panel d) of figure 1 where the intensity on the detector is plotted as a function of time for a given q. The sharp peaks in the intensity are in this case due to unequally long acquisition times.